Anthropologica et Præhistorica, 126/2015 (2016) : 57-67

Assessing apatite cathodoluminescence as a tool for sourcing oolitic ironstones

Jean-Marc BAELE, Roland DREESEN & Michiel DUSAR

Résumé

La cathodoluminescence (CL) est un processus au cours duquel de la lumière visible est émise par des minéraux lorsqu'ils sont bombardés par un faisceau d'électrons énergétiques. Des défauts cristallins et des impuretés chimiques peuvent soit activer ou inhiber la CL en fonction de leur nature et de leur concentration. Mn^{2+}, Ti^{4+}, Fe^{3+}, Cr^{3+}, Eu^{2+} and REE^{3+} (terres rares) sont des exemples d'activateurs dans beaucoup de minéraux tandis que Fe^{2+} est un inhibiteur courant. De légères variations dans la composition en éléments en traces ou en défauts cristallins mènent fréquemment à un changement très notable de l'émission CL, qui peut alors être utilisée comme une empreinte génétique dans les problèmes de provenance. Une émission CL intense et colorée est presque omniprésente dans l'apatite, qui est un minéral accessoire très commun dans les oolites ferrugineuses. La raison est que l'apatite est un bon piège pour Mn^{2+} et les terres rares (qui sont activateurs de la CL) mais pas pour Fe^{2+} (qui est inhibiteur).

Nous documentons ici l'étude d'oolites ferrigineuses du Dévonien supérieur de Saint-Ghislain, Vezin-Sclaigneaux, Couthuin, Aisémont et Boosichot (Belgique). Nous avons trouvé des différences significatives en ce qui concerne le cathodofaciès et l'émission spectrale du phosphate de calcium dans ces roches, qui pourraient être utilisées pour retrouver les zones d'approvisionnement de ces matériaux. Dans l'oolite ferrugineuse, le phosphate de calcium se présente sous la forme 1) d'une masse fine et disséminée, 2) de dépôts diagénétiques dans les vides de la roche et en remplacement de minéraux déjà présents, 3) de lamines d'oolites, 4) de bioclastes (dont des conodontes), et, moins fréquemment 5), de grains détritiques. L'apatite diagénétique montre la plus grande variabilité des caractéristiques de CL. À Saint-Ghislain, elle présente une séquence diagénétique complexe qui consiste en une phase à CL rose à bleue suivie de phases rouge, jaune, vert-bleu et vert. À Couthuin, la sequence est moins complexe et consiste en une phase à CL bleue suivie d'une phase orange à rose. À Vezin, une séquence similaire est observée à l'exception d'une phase intermédiaire verte. De plus, l'apatite s'y trouve préférentiellement en remplacement de feldspaths, l'espace intergranulaire étant plutôt occupé par du quartz et/ou de la calcite diagénétiques. À Aisémont, l'apatite se trouve dans des lamines d'oolithe et en remplacement de bioclastes calcaires. Elle y montre une luminescence bleu profond qui peut se changer en vert sans qu'il y ait de véritable séquence chronologique de dépôt. Un échantillon d'oolite ferrugineuse standard provenant de l'Alabama, Etats-Unis, a également été étudié à titre de comparaison. Aucune séquence diagénétique nette n'a été reconnue mais l'apatite montre une luminescence vert pâle significativement différente des autres.

Nos résultats montrent que tous les échantillons analysés peuvent être distingués sur base de leurs caractéristiques CL. Cette technique pourrait donc fournir une signature unique et peut dès lors être considérée comme un outil puissant pour l'analyse de provenance des oolithes ferrugineuses et d'autres matériaux. Elle supplémente les autres techniques conventionnelles comme la microscopie optique et électronique tout en faisant le lien entre la pétrographie et la géochimie.

Mots-clés : *Cathodoluminescence, apatite, oolite ferrugineuse, Dévonien, Belgique, provenance.*

Keywords: Cathodoluminescence, apatite, oolitic ironstone, Devonian, Belgium, sourcing.

1 INTRODUCTION

Many minerals emit light when they are subjected to bombardment by electrons accelerated with a voltage typically in the 10-20 kV range (Marshall, 1988; Pagel *et al.*, 2000; Götze & Kempe, 2009). This phenomenon, called cathodoluminescence (CL), is caused by several luminescence centres consisting of defects and chemical impurities at the ppm (part per million) level within the crystal lattice. Chemical impurities such as Mn^{2+}, Ti^{4+}, Fe^{3+}, Cr^{3+}, Eu^{2+} and REE^{3+} causing CL emission are *activators* whereas other such as Fe^{2+} and Co^{2+}, which lower or suppress CL, are *inhibitors*. The

CL emission is very sensitive to slight variations in defects and trace element concentrations, which may be used as a fingerprint for sourcing natural and manufactured geomaterials.

Apatite very often shows bright CL emission since Mn^{2+}, Eu^{2+} and REE^{3+} (activators) ubiquitously substitute for Ca^{2+} in the crystal lattice whereas Fe^{2+} (quencher) does not. Several CL emission colors are observed depending on the activators. Mn^{2+} activation results in yellow-green CL, while REE (mainly Eu^{2+}, Dy^{3+}, Sm^{3+}) induces violet, blue, green to red CL colors (Waychunas, 2002).

Apatite is an extremely common accessory mineral in oolitic ironstones, occurring in the mineralogical form carbonate-apatite, or francolite (Karakus *et al.*, 1988). Phosphorus in these rocks was probably adsorbed onto and incorporated in the primary iron oxide precipitates (ferrihydrite) and subsequently released in pore fluids as ferrihydrite stabilized into more stable minerals (goethite and hematite) as shown in hydrothermal sediments in the East Pacific Rise (Poulton & Canfield, 2006). Ferrihydrite precipitating in iron microbial mats in freshwater environments systematically contains significant amounts of phosphorus (Papier, 2014). Due to this high affinity of phosphorus for iron oxides, it is highly probable that virtually all oolitic ironstones will contain at least trace amounts of apatite, depending on calcium availability during diagenesis.

Oolitic ironstone samples from 6 localities were studied in order to evaluate apatite cathodoluminescence as a potential tool for sourcing archaeological materials. As a first step in our approach, only source materials were considered in order to investigate the variability of the CL characteristics of ironstones.

2 MATERIALS AND METHODS

Samples for this study were taken from boreholes cores (Saint-Ghislain and Booischot) and from former ironstone mines in Belgium (Vezin-Sclaigneaux, Couthuin and Aisémont), provided by the rock library (lithotheque) of the Geological Survey of Belgium. All these ironstones are of Upper Devonian (Famennian) age. One sample from Alabama, USA (Krantz rock collection), which is a famous locality for ordovician oolitic ironstone, was also selected for comparison. Polished thin-sections were prepared from these samples, >100 for Saint-Ghislain (partly studied in Etienne, 2010), 12 for Vezin and 1 to 2 for the other localities. The idea behind the large number of thin-sections for Saint-Ghislain and Vezin was to test the variability of the CL characteristics within the same locality.

The thin-sections were studied under the polarizing microscope to examine the mineralogy and the petrography of the ironstones. They were then investigated under cathodoluminescence (CL) using a cold-cathode CITL Mk5 unit operated at an acceleration voltage and beam current of 15 kV and 500 µA, respectively (defocussed beam). The unit is mounted on a Zeiss Universal-R microscope customized for spectroscopy and spectral imaging using a CITL OSA2 optical spectrometer (380-1100 nm spectral range) and a set of bandpass interference filters. Spectroscopy was used to identify the CL activators to differentiate those minerals with similar emission color. CL micrographs at high magnification were acquired with an optical digital camera fitted on a Cameca SX50 electron microprobe (hot-cathode, or SEM-CL) operated at 15 kV and 20 nA (focused beam, scanned). A 20 nm-thick conductive coating (carbon) was applied onto the thin-sections. A very good correspondence was observed between the CL colors obtained with the cold- and hot-cathode equipments.

3 MINERALOGY AND PETROGRAPHY

All the investigated ironstone samples consist of grains with a size ranging from a few hundreds of micrometer to 1 millimeter. The grains are predominantly ooids with a typical concentric structure made of thin laminae. A nucleus, i.e. the former grain onto which laminae successively deposited during ooid formation, is sometimes visible. The ooids are more or less flattened and composed of iron minerals, mainly hematite, goethite and chlorite (chamosite). A few laminae may be composed of phosphate but they are better identifiable under CL (see below). Other grains consist of calcareous and phosphatic bioclasts, and detrital minerals: quartz, feldspars, muscovite, apatite and zircon. Many phosphatic grains are unidentifiable and probably represent coprolites, pellets, phosphatized grains of unknown origin

and clasts of phosphatic skeletons. Also, conodonts are common phosphatic bioclasts that are easily recognizable by their typical morphology and CL color. Fine-grained clayey or phosphatic sediment may be observed as well.

The grains in ironstones are bound together by a diagenetic cement, which consists of irons oxides, apatite, quartz and/or carbonate (calcite, dolomite, ankerite and siderite). Such diagenetic minerals are usually deposited in voids but they are also found replacing the grains, which may obscure the original texture of the ironstone. Phyllosilicates (illite/muscovite) are also present as replacement of former minerals, especially in Saint-Ghislain. Sulphides, chiefly pyrite but also galena and sphalerite, and sulphates, anhydrite and strontianite, were observed in minor amounts, except in Vezin, where the ironstone may be pervasively replaced by pyrite, probably due to the flow of H_2S-rich fluids along fractures during late diagenesis, as reported in Brittany by Gloaguen *et al.* (2007).

4 CATHODOLUMINESCENCE

4.1 General CL characteristics

Amongst the minerals in the oolitic ironstones listed above, only apatite, feldspars, calcite, dolomite, quartz and zircon are luminescing. Zircon is a ubiquitous accessory mineral in many sedimentary rocks and its CL characteristics will not be discussed here.

4.1.1 Apatite

Apatite in the investigated ironstones showed a great variety of CL emission colors. Rare detrital apatite exhibits a very bright yellow-green emission at 575 nm due to Mn^{2+} activation (Fig. 1).

In diagenetic apatite, REE activation superimposes onto this emission, yielding a wide range of colors depending on the dominant REE and other factors yet unknown. Samples from Saint-Ghislain, Couthuin and Vezin were studied under spectroscopy in order to establish the link between emission spectra and the resulting colors. A blue-dominated CL color is caused by a broad band emission at ca. 420 nm caused by Eu^{2+} (Pagel *et al.*, 2000; Waychunas, 2002), which is frequently observed in Couthuin and Vezin but rarely in Saint-Ghislain, where the occasional blue CL color rather appears to result from a strong Dy^{3+} sharp emission at 485 and 585 nm. Mn^{2+} activation superimposed onto this emission adds a green component and the resulting color is distinct from the "pure" yellow-green due to Mn activation alone. An orange-red CL color may originate from Sm^{3+} activation at 605 and 645 nm lines but the possible influence of an unknown, additional broad band emission in the red region is currently under investigation. This emission cannot be separated from the main Mn-activation at 575 nm, which simply appears more asymmetrical towards longer wavelengths. It yields the typical yellow and red-luminescing diagenetic apatite in the Saint-Ghislain and Vezin apatite. These yellow and red emissions are probably the result of Mn activation as well but in a different crystal field due to change in apatite chemistry, as suggested by Baele *et al.*, 2011 for hydroxyapatite in fossil bones. All other shades of CL emission are the result of a mixed influence of the above activators, a more or less equilibrated mix resulting in a grey to white emission.

Neodymium activation occurs at ca. 870 nm, i.e. in the near-infrared region of the spectrum, which therefore, cannot produce any visible color. However, CCD (couple-charged-device) cameras are sensitive to such emission providing they have no IR-blocking filter mounted in front of the sensor.

4.1.2 Feldspars and quartz

Feldspars exhibit diverse CL color due to the combination of a series of activators (Eu^{2+}, Ti^{4+}, Mn^{2+}, Fe^{3+} to name the most important; Marshall, 1988; Pagel *et al.*, 2000) as does quartz, but with an much lower overall intensity. Common CL colors of feldspars are blue for orthoclase and yellow to reddish-brown for plagioclase. Quartz is usually blue to violet (magmatic origin) or brown (metamorphic). The details on CL activation of these minerals will not be given here but can be found in e.g. Marshall (1988).

4.1.3 Calcite and dolomite

Calcite and dolomite are very commonly activated by Mn^{2+} substituting for Ca^{2+} and/or Mg^{2+} and this gives rise to a unique broad band emission in the yellow-red region of the spectrum (Machel, 1985). Due to the different crystal lattice environment in calcite and dolomite, which

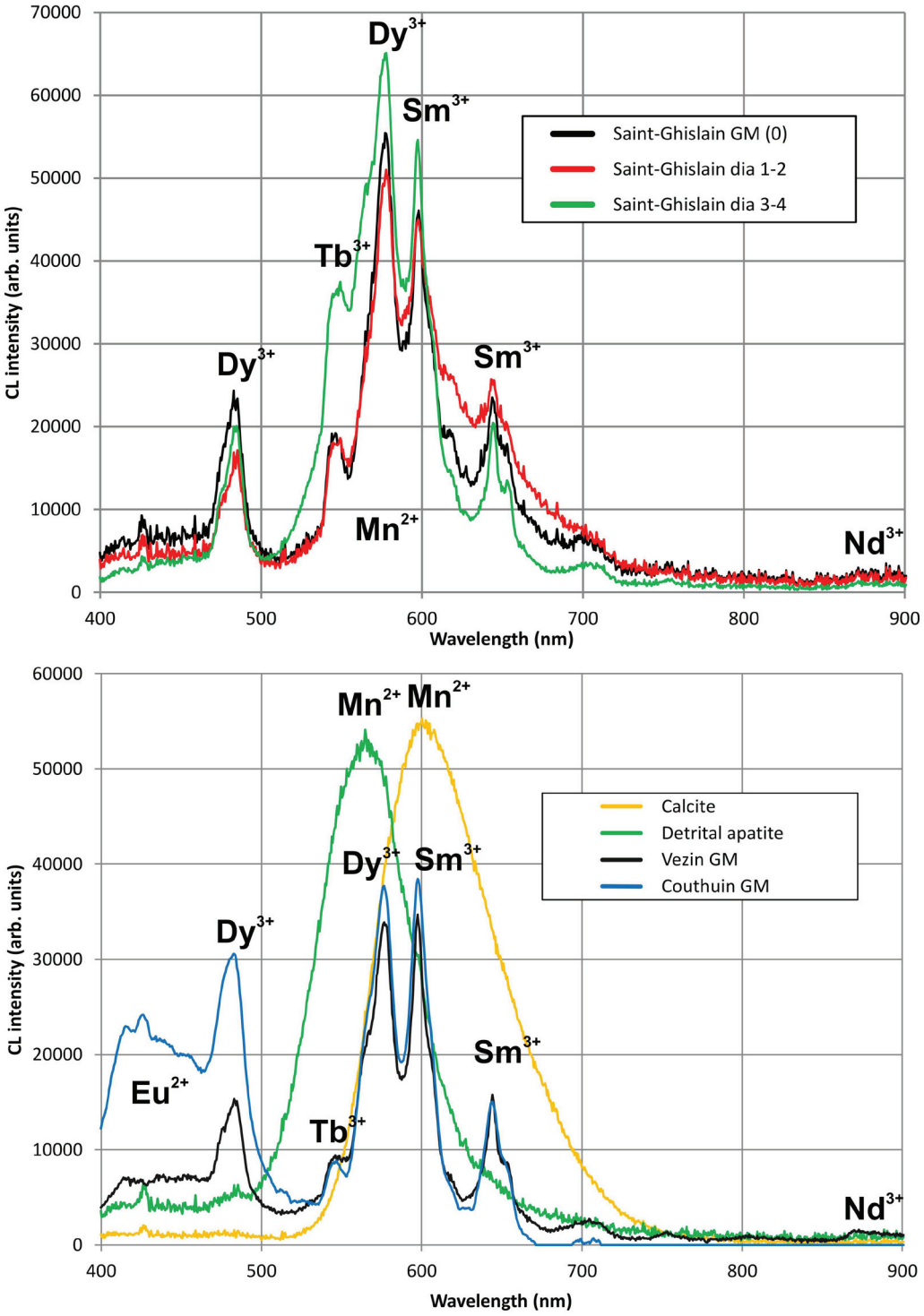

Fig. 1 – Cathodoluminescence (CL) emission spectra of apatite and calcite in Upper Devonian oolitic ironstones from Belgium. Upper graph: spectra of the Saint-Ghislain samples. GM = groundmass apatite (stage 0), dia = diagenetic apatite (corresponding diagenetic stage indicated). Lower graph: spectra from Vezin and Couthuin. The main CL activators are indicated.

Fig. 1 – *Spectres d'émission de cathodoluminescence (CL) d'apatites et de calcite dans des oolites ferrugineuses du Dévonien Supérieur de Belgique. Graphe en haut : spectres relatifs à Saint-Ghislain. GM = apatite disséminée (phase 0), dia = apatite diagénétique (la phase correspondante est mentionnée). Graphe en bas : spectres relatifs à Vezin et Couthuin. Les activateurs principaux de la CL sont indiqués.*

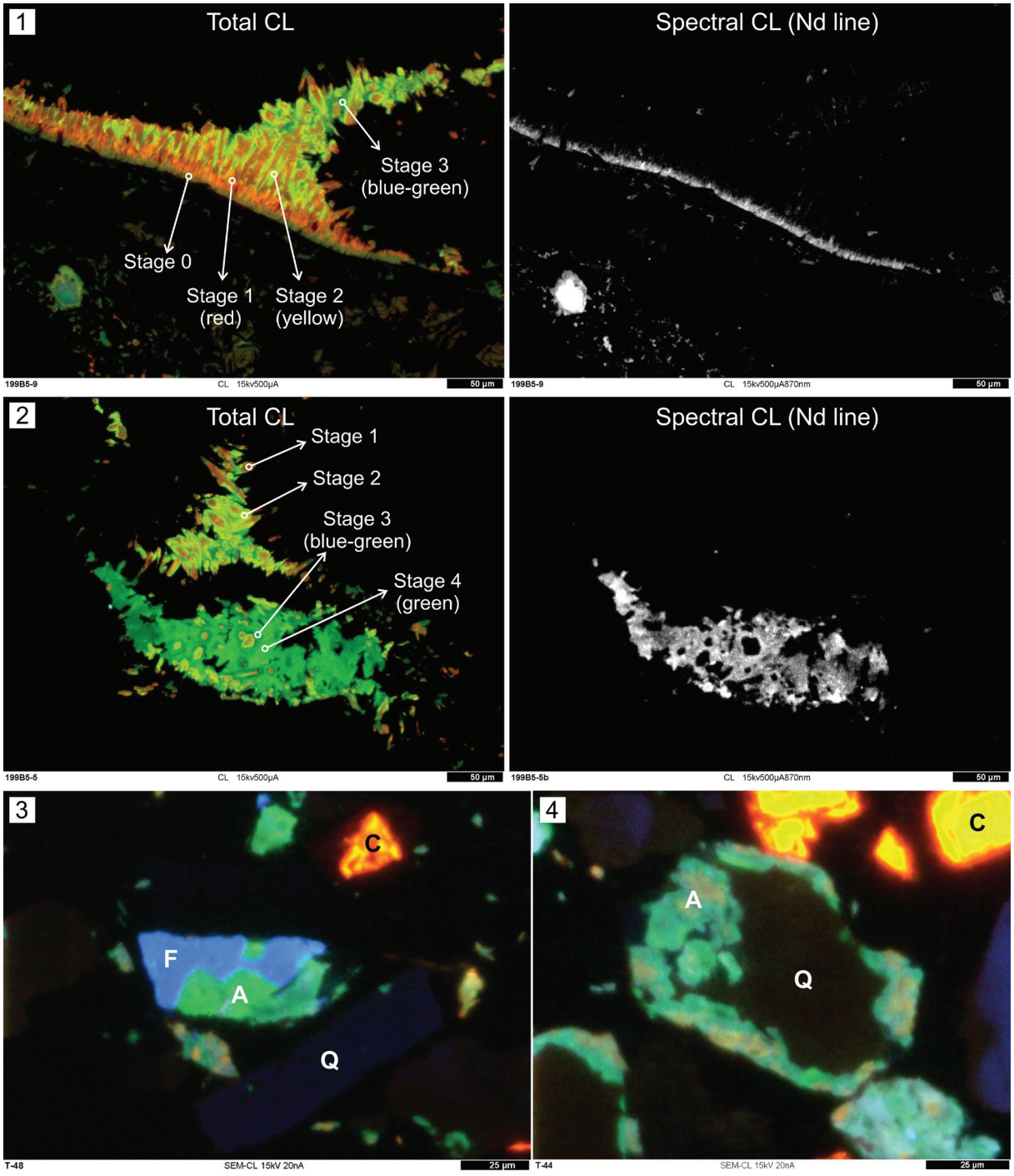

Fig. 2 – Cathodoluminescence imaging of apatite in the Saint-Ghislain ironstone. Photos 1 and 2 depict the diagenetic sequence in total (left) and spectral (right) CL (optical CL, scale bar 50 µm). The latter show the distribution of neodymium, which is not visible in total CL because it occurs in the near-infrared. In photos 3 and 4, apatite is replacing feldspars and quartz grains (SEM-CL, scale bar 25 µm). F = feldspar, Q= quartz, A = apatite and C = calcite.

Fig. 2 *– Imagerie de cathodoluminescence de l'apatite de l'oolithe ferrugineuse de Saint-Ghislain. Les photos 1 et 2 montrent la séquence diagénétique en CL totale (à gauche) et spectrale (à droite) (CL optique, échelle = 50 µm). L'imagerie spectrale permet de visualiser la distribution du néodyme, qui n'est pas visible en Cl totale puisqu'elle se produit dans le proche-infra-rouge. Dans les photos 3 et 4, l'apatite remplace les grains de feldspath et de quartz (CL sous microsonde électronique, échelle = 25 µm). F = feldspath, Q = quartz, A = apatite et C = calcite.*

influences the electronic levels of the activator, and the existence of two substituting sites in dolomite, the same Mn-activation produces a yellow and red CL color in calcite and dolomite respectively (although dolomite may rarely exhibit yellow or green CL; Gillaus *et al.*, 2010).

Spectral imaging of the neodymium emission provided an effective means of quickly distinguishing apatite and calcite with similar CL color since neodymium does not, or very uncommonly, activate the CL of calcite.

4.2 CL characteristics by locality

4.2.1 Saint-Ghislain

The main CL characteristics of apatite in the Saint-Ghislain ironstone lies in a complex

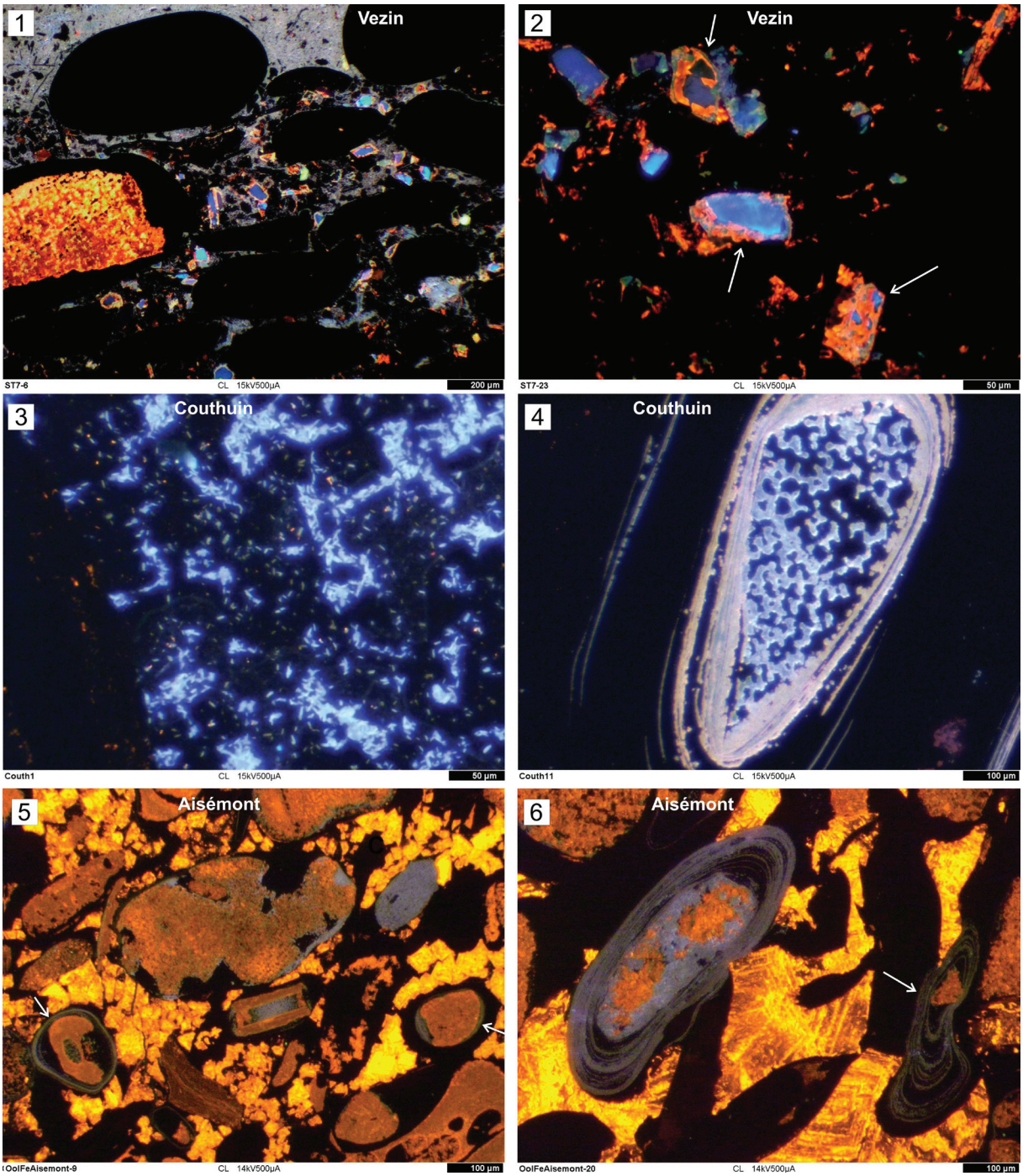

diagenetic sequence, which is observed in virtually all samples. The sequence starts with fine-grained apatite with a pinkish to blueish CL of moderate intensity, mainly activated by REE^{3+} (stage 0). This apatite was obviously part of a fine-grained sediment or early precipitates. It is overgrown by needle-like apatite crystals comprising a four-stage CL sequence with a bright luminescence: 1) red, 2) yellow, 3) blue-green and 4) green (Fig. 2). Apatites in stage 0 and 4 are predominantly REE-activated as shown by spectra and spectral imaging of neodymium. In contrast, stage 1, 2 and 3, are predominantly Mn-activated. Crystal morphology also seems to change from acicular to equigranular in stage 4. This diagenetic sequence is observed in intergranular (i.e. having been deposited in the voids between the oolites) but also intragranular apatite, specifically in nuclei that are interpreted as former carbonate grains that were dissolved before apatite precipitated. Diagenetic apatite is also observed overgrowing conodonts and other phosphate grains as well as replacing K-feldspar (but not plagioclases) and quartz grains. Feldspar grains frequently have a rhombic shape, suggesting a possible volcanic origin, corroborating the volcanogenic source of the iron in Palaeozoic oolitic ironstones (Dreesen, 1989; Sturesson *et al.*, 1999; 2000).

Apatite in grains and oolite laminae exhibits a moderate CL of brownish color produced by both REE and Mn-activation. Many flakes of non-luminescing muscovite-illite of diagenetic origin are present.

Carbonates are very rare in Saint-Ghislain. Dolomite rhombs were occasionally observed in samples enriched in detrital minerals that are believed to represent the transition rock between the ironstone and adjacent formations.

4.2.2 Vezin-Sclaigneaux

In Vezin, diagenetic apatite is observed as a fine groundmass with a greyish- to blueish white CL (fig. 3). It is followed by green then orange-red apatite. Similarily to Saint-Ghislain, diagenetic apatite is found replacing rhombic K-feldspars. The apatite sequence is thus less complex than in Saint-Ghislain. Additionaly, it is rarely observed in intergranular pores, but rather as replacement. This porosity is now filled with quartz which contains calcite inclusions, indicating the silicification of a former carbonate cement.

Diagenetic apatite in ooid laminae and phosphatized grains exhibits a blueish-white to greenish CL color distinct from its counterpart in the Saint-Ghislain ironstone.

Fig. 3 – (belows cons) Cathodoluminescence imaging of apatite in the Vezin (1-2), Couthuin (3-4) and Aisémont (5-6) ironstones. In photo 1, the white-luminescing groundmass apatite is visible in the upper part. Note the yellow-red luminescing calcitic nucleus on the left. Photo 2 shows a close-up of rhombic K-feldspars being partially replaced by apatite (arrows). Photo 3 shows the fine-grained apatite groundmass with a bacillus-like morphology. Note the dark rhombs corresponding to non-luminescing carbonates. In photo 4, a crinoid now replaced by blue-luminescing apatite served as nucleus for ooid formation, starting with pink-luminescing apatite laminae. Note in photos 5 and 6 the abundance of yellow-luminescing, zoned calcite. Apatite, mainly in ooid laminae, is deep blue-luminescing with some green-luminescing zones (arrows). Scale bars: 1 = 200 µm, 2 and 3 = 50 µm, 4, 5 and 6 = 100 µm.

Fig. 3 *– (ci-contre) Imagerie de cathodoluminescence de l'apatite dans les oolites ferrugineuses de Vezin (1-2), Couthuin (3 et 4) et Aisémont (5 et 6). Dans la photo 1, l'apatite finement disséminée luminescente en blanc est visible dans la partie supérieure. Noter le nucleus d'oolite en calcite luminescente en jaune-rouge à gauche. La photo 2 montre un agrandissement de feldspaths potassiques rhombiques partiellement remplacés par de l'apatite (flèches). La photo 3 montre la morphologie « en bacilles » de l'apatite finement disséminée. Noter les formes rhombiques sombres qui correspondent à des carbonates non-luminescents. Dans la photo 4, un bioclaste de crinoïde maintenant remplacé par de l'apatite à luminescence bleue a servi de nucleus pour la formation d'une oolite, qui débute par des lamines d'apatite luminescentes en rose. Noter, dans les photos 5 et 6, l'abondance de la calcite zonée luminescente en jaune. L'apatite, présente ici principalement dans les lamines des oolites est luminescente en bleu avec quelques zones vertes (flèches). Barres d'échelle : 1 = 200 µm, 2 and 3 = 50 µm, 4, 5 and 6 = 100 µm.*

Conodont bioclasts have a dark-green emission resulting from a combined REE and Mn-activation in which the latter predominates. However, conodonts in Vezin often exhibit a distinct blueish shade consistent with the Eu^{2+} emission observed in diagenetic apatite from this locality. Consistently, a few conodonts with a red component in their emission were observed in Saint-Ghislain.

Calcite is rather common in Vezin, especially as vein-fill.

4.2.3 Couthuin

In Couthuin, the fine-grained apatite in the groundmass has a blueish-white CL and a typical bacillus-like morphology due to the presence of minute scattered apatite crystals of a few

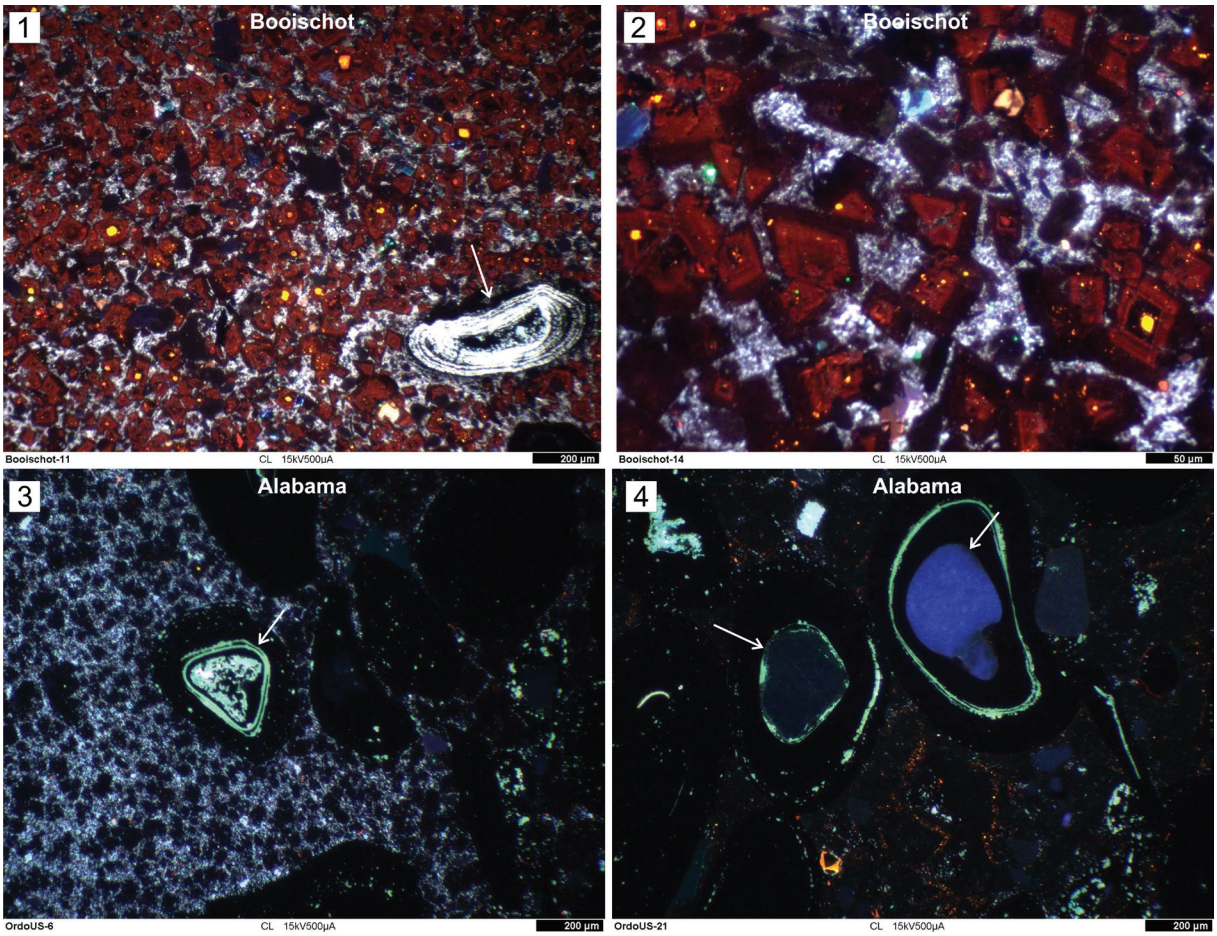

Fig. 4 – Cathodoluminescence imaging of selected Booischot (1-2) and Alabama (3-4) oolitic ironstone samples. In photo 1 apatite within the fine-grained groundmass and ooid laminae is white-luminescing. The close-up in photo 2 shows the details of the groundmass and the red-brown luminescing dolomite rhombs. Photos 3 and 4 depict the cathodofacies of the Alabama oolitic ironstone which comprises fine-grained groundmass apatite with non-luminescing carbonates (dark spots in 3). Light-green luminescing apatite occasionally occurs within the ooid laminae and the nucleus. Note the presence of well-rounded quartz grains as ooid nuclei (arrows in 4). Scale bars: 1-3 and 4 : 200 µm, 2: 50 µm.

Fig. 4 *– Imagerie de cathodoluminescence des échantillons sélectionnés d'oolite ferrugineuse de Booischot (1-2) et de l'Alabama (3-4). Dans la photo 1, l'apatite formant la masse finement disséminée et des lamines dans les oolithes est luminescente en blanc. L'agrandissement dans la photo 2 montre le détail de cette masse ainsi que les rhomboèdres de dolomite à luminescence brun-rouge zonée. Les photos 3 et 4 illustrent le cathodofaciès de l'oolite de l'Alabama, qui comprend une masse finement disséminée parsemée de carbonates non-luminescents (taches sombres dans la photo 3). De l'apatite à luminescence vert pâle est parfois présente dans les lamines et les nuclei des oolites (flèche). Noter les nuclei formés de grains de quartz bien arrondis (flèche dans la photo 4). Barres d'échelle : 1-3 et 4 : 200 µm, 2 : 50 µm.*

micrometers in size (Fig. 3). Diagenetic apatite mainly occurs as ooid laminae and replacement of bioclasts (crinoids, bryozoa, etc.) The sequence recognized so far is blue-CL followed by orange-CL apatite, the latter emission color being perceived more pinkish than reddish due to a blue component as detected by spectroscopy.

Non-luminescing (Fe^{2+}-rich) carbonate rhombs are scattered in the groundmass and they contain a few bacillus -like apatite inclusions. Rare brown-luminescing calcite laminae or fracture fillings were observed.

4.2.4 Aisémont

Diagenetic apatite in the Aisémont ironstone is concentrated in the ooid laminae and calcareous bioclasts (fig. 3). Two distinct emission colors are observed: deep blue and green, both with a moderate luminescence intensity. There is no clear sequence as the CL color may change across the same ooid laminae.

Bright luminescing calcite is very abundant in the Aisémont samples. Conventional petrography shows many iron oxides inclusions in zoned calcite, which suggests that this iron was originally dissolved as Fe^{2+} in the calcite lattice, after which it was oxidized and exsolved out of carbonate, thus allowing Mn^{2+}-activated luminescence.

4.2.5 Booischot

The sample from Booischot showed bright blueish-white to white-luminescing diagenetic apatite in a fine-grained groundmass and in oolite laminae (Fig. 4). There are many reddish-brown luminescing, zoned dolomite rhombs scattered throughout the cement. These rhombs have no apatite inclusions, but yellow-luminescing calcite.

4.2.5 Alabama

In the ironstone sample from Alabama, diagenetic apatite is ubiquitously light-green luminescing although the bacillus -like groundmass exhibits a more light CL color (Fig. 4). Non-luminescing carbonate rhombs with no apatite inclusions are present.

Detrital quartz is common and the grains are very well-rounded. In addition, they are often found as nuclei in the ooids.

Traces of brown-luminescing calcite may be observed.

Locality	*Carbonate*	*Detritals*	*Diagenetic apatite*		
			*CL Sequence**	*CL Colors*	*Replacement***
Saint-Ghislain	rare (D)	K, P & Q	unique, 5-stage	Pink/blue -> red -> yellow -> blue-green -> green	K and Q
Vezin-Sclaign	C+D	K & Q	unique, 3-stage	Blue -> green -> orange	K
Couthuin	(NL)	Q	unique, 2-stage	Blue -> orange (pink)	-
Aisemont	C (zoned)	very rare	No	Blue <-> dark-green	-
Booischot	D (zoned)	Q (K & P)	No	Blueish-white	-
Alabama	rare (incl. C)	Q	No	Light green	-

C: calcite D: dolomite K: K-feldspar P: plagioclase Q: quartz NL: non-luminescing
*Subsequent to fine-grained groundmass with bacillus-like crystals
**Excluding calcareous bioclasts

Tab. 1 – Summary of the distinguishing features provided by cathodoluminescence analysis of the selected oolitic ironstone samples. All the samples can be distinguished based on these features. See text for additional features and further explanation.

Tab. 1 *– Résumé des caractéristiques distinctives fournies par l'analyse en cathodoluminescence des échantillons d'oolite ferrugineuse sélectionnés. Ces caractéristiques permettent de distinguer tous les échantillons entre eux. Se reporter au texte pour d'autres caractéristiques et plus d'explications.*

5 DISCUSSION

Based on the observed characteristics in the studied samples (Tab. 1), the diagenetic apatite sequence appears as the most distinguishing feature. The apatite sequence commonly starts with a blue CL zone and ends with green or orange CL overgrowths, indicating some common trend in the temporal change in composition of the diagenetic fluids. However, in detail, the sequence is significantly different from one locality to another and reflects a unique history of the sediments in the basin or a particular region thereof. The diagenetic apatite sequence can thus be regarded as a real fingerprint. Other observations such as the blue Eu^{2+} emission in samples from Couthuin and Vezin, the well-rounded quartz grains in Alabama, the CL of the diagenetic quartz (not presented here) could also be used as additional distinguishing features along with other classical mineralogical and petrographical characteristics (see for instance Dreesen *et al.*, 2016: this volume). Besides changes in initial sediment composition, the assemblage and growth history of diagenetic minerals such as apatite can therefore be quickly examined with CL analysis. However, in provenance studies, it is important to first evaluate the variation of the characteristics within the same locality before attempting to compare with other localities. Here, this evaluation was conducted only for samples from Saint-Ghislain and Vezin, which both yielded uniform signatures. All of the >100 samples from Saint-Ghislain exhibit the same diagenetic apatite sequence, which is significantly different from the samples from other localities, even if they are stratigraphically almost analogous. Yet more samples from the other localities, where only one or two thin-sections were studied should be investigated in the future in order to evaluate the uniformity of the diagenetic apatite sequence.

6 CONCLUSION

All of the investigated samples can be distinguished based on their CL characteristics, which are here considered as diagnostic features or fingerprints. Apatite is especially interesting since it is a very common accessory mineral in oolitic ironstones. This mineral readily incorporates during diagenesis those trace-elements which act as CL activator (REE and Mn^{2+}), but not inhibitors (Fe^{2+}). The relative abundance of these trace-elements is reflected by the emission intensity and color of apatite. Our results show that CL imaging of apatite is an efficient tool in provenance analysis. More complex techniques such as spectroscopy and spectral imaging provide additional information and allow distinguishing minerals with similar CL color.

Although focused on apatite, this study also shows other luminescing minerals that are difficult to observe under conventional optical microscopy, mainly feldspars and carbonate when they are present at trace amounts, are revealed with CL. This technique may therefore be considered as a valuable tool for sourcing ironstones and other natural or manufactured geomaterials in complement with other techniques such as conventional optical and electron microscopy. Due to its high sensitivity to trace-elements, CL also bridges the gap between petrography and geochemistry.

Bibliography

BAELE J. M., PAPIER S., BARRIQUAND L., & BARRIQUAND J., 2011. Insights into the use of cathodoluminescence for bone taphonomy in the fossil bear deposit of Azé Cave, Saône-et-Loire, France. *Quaternaire*, Hors-série, **4**: 291-296.

DREESEN R., 1989. Oolitic ironstones as event-stratigraphical marker beds within the Upper Devonian of the Ardenno-Rhenish Massif. In: T. P. YOUNG & W.E.G. TAYLOR (ed.), Phanerozoic Ironstones. London, Geological Society Special Publication **46**: 65-78.

DREESEN R., SAVARY X. & GOEMAERE É., 2016. Definition, classification and microfacies characteristics of oolitic ironstones, used in the manufacturing of red ochre - a comparative petrographical analysis of Palaeozoic samples from France, Belgium and Germany. *In*: C. BILLARD *et al.* (ed.), *Autour de l'hématite / About haematite. Actes de / Acts of Jambes, 7-8/02/2013, Volume 1*, Liège, ERAUL, **143** - *Anthropologica et Præhistorica*, **125/2014:** 203-223.

ETIENNE A., 2010. *Minéralogie, diagenèse et environnement de formation de l'hématite oolithique du sondage de Saint-Ghislain*. Unpublished Master Thesis, University of Mons, Mons.

GILLAUS A., RICHTER D. K., GÖTTE Th. & NEUSER R. D., 2010. From tabular to rhombohedral dolomite crystals in Zechstein 2 dolostones from Scharzfeld (SW Harz/Germany): A case study with combined CL and EBSD investigations. *Sedimentary Geology*, **228**: 284-291.

GLOAGUEN E., BRANQUET Y., BOULVAIS Ph., MOËLO Y., CHAUVEL J. J., CIAPPERO P.J. & MARCOUX E., 2007. Palaeozoic oolitic ironstone of the French Armorican Massif: a chemical and structural trap for orogenic base metal–As–Sb–Au mineralisation during Hercynian strike-slip deformation. *Mineralium Deposita*, **42** (4): 399-422.

GÖTZE J., & KEMPE U., 2009. Physical principles of cathodoluminescence (CL) and its applications in Geosciences. In: A. GUCSIK (ed.), *Cathodoluminescence and its application in the planetary sciences*. Berlin Heidelberg, Springer-Verlag: 1-22.

KARAKUS M., HAGNI R. D., & SPRENG A. C., 1988. Cathodoluminescence petrography of phosphate grains in Jurassic (Aalenian) sedimentary iron ores, Alsace-Lorraine, France. *Proceedings of the 22nd Annual Meeting of the Geological Society of America, North-Central Section*, **20** (5): 351.

MACHEL H. G., 1985. Cathodoluminescence of calcite and dolomite and its geochemical interpretation. *Geoscience Canada*, **12** (4): 139-147.

MARSHALL D. J. (ed.), 1988. *Cathodoluminescence of Geological Materials*. Boston, Unwin Hyman.

PAGEL M., BARBIN V., BLANC P. & OHNENSTETTER D. (ed.), 2000. *Cathodoluminescence in Geosciences*. Berlin, Heidelberg, Springer-Verlag.

PAPIER S., 2014. *Géomicrobiologie des dépôts bactériens ferrugineux : influence des facteurs biologiques et environnementaux sur l'oxydation du fer en milieu continental*. PhD thesis, University of Mons, Mons.

POULTON S. W. & CANFIELD D. E., 2006. Co-diagenesis of iron and phosphorus in hydrothermal sediments from the southern East Pacific Rise: implications for the evaluation of paleoseawater phosphate concentrations. *Geochimica et Cosmochimica Acta*, **70**: 5883-5898.

STURESSON U., DRONOV A. & SAADRE T., 1999. Lower Ordovician iron ooids and associated oolitic clays in Russia and Estonia: a clue to the origin of iron oolites? *Sedimentary Geology*, **123**: 63-80.

STURESSON U., HEIKOOP J. M. & RISK M. J., 2000. Modern and Palaeozoic iron ooids - a similar volcanic origin. *Sedimentary Geology*, **136**: 137-146.

WAYCHUNAS G. A., 2002. Apatite luminescence. *Reviews in Mineralogy and Geochemistry*. **48**: 701-741.

Authros address:

Jean-Marc BAELE
Department of Geology
Faculty of Engineering
University of Mons
20, Place du Parc
7000 Mons (Belgium)
jean-marc.baele@umons.ac.be

Roland DREESEN
Michiel DUSAR
Royal Belgian Institute of Natural Sciences
Belgian Geological Survey
13, Jennerstreet
1000 Brussels (Belgium)
roland.dreesen@telenet.be